ELSEVIER

Chemical Geology 237 (2007) 418–432

CHEMICAL GEOLOGY
INCLUDING
ISOTOPE GEOSCIENCE

www.elsevier.com/locate/chemgeo

# Geochemistry of melt inclusions from the Fondo Riccio and Minopoli 1 eruptions at Campi Flegrei (Italy)

C. Cannatelli [a,b,*], A. Lima [a], R.J. Bodnar [b], B. De Vivo [a], J.D. Webster [c], L. Fedele [a]

[a] *Università di Napoli Federico II, Dipartimento di Scienze della Terra, Naples, Italy*
[b] *Virginia Polytechnic Institute & State University, Department of Geosciences, Blacksburg, VA, USA*
[c] *American Museum Natural History, New York, USA*

Accepted 10 July 2006

Editor: R.L. Rudnick

**Abstract**

Campi Flegrei is a large volcanic complex (~ 150 $km^2$) located west of the city of Naples, Italy. The area has been the site of volcanic activity for more than 60,000 years and represents a potential volcanic hazard owing to the large local population. In this study, the geochemistry of the magma associated with two different eruptions at Campi Flegrei has been characterized, with the aim to identify geochemical trends that may help to predict the style and nature of future eruptions. Two eruptions of different age and eruptive style have been selected for study, Fondo Riccio (9.5 ka) and Minopoli 1 (11.1 ka). A scoria (CF-FR-C1) and a bomb (CF-FR-C2) were collected from the Fondo Riccio eruption, and two scoria samples were collected from the Minopoli 1 (CF-Mi1-C1 and C2) eruptive products.

The pre-eruptive volatile content of magma plays an important role in the style of eruption. The original volatile content of magma can be assessed from studies of melt inclusion (MI) contained in phenocrysts. MI data show two trends for Fondo Riccio – one from latite to trachyte for MI in Fe-rich diopside (C1) and another from trachybasalt to shoshonite for MI in Mg-rich diopside (C2) and for MI in olivine (C1). Minopoli 1 MI data show two different compositions – basaltic for MI in clinopyroxene (Mi1-C1) and trachybasalt for MI in olivine (Mi1-C1) and clinopyroxene (Mi1-C2). Major and trace element data for Fondo Riccio MI show a compositional gap between Mg# 78 and 83, whereas Minopoli 1 MI have Mg# between 85 and 89 and show no compositional gap. Clinopyroxene compositions fall in the diopside–salite field for Fondo Riccio and in the diopside field for Minopoli 1. Fondo Riccio olivine compositions show a wider range ($Fo_{84.60}$ to $Fo_{86.77}$), compared to Minopoli 1 olivine ($Fo_{77}$ to $Fo_{78.5}$). Analyses of reheated MI suggest trends in MI volatile contents that correlate with $SiO_2$ concentration. In particular, more evolved MI show higher Cl and lower S compared to less evolved MI. The $H_2O$ content of MI from the two eruptions overlap but suggest that the Fondo Riccio magma may have been more water-rich. The higher $H_2O$ content of the Fondo Riccio magma (2.5 to 6.9 wt.%) compared to Minopoli 1 (1–3.5 wt.%) is consistent with the more explosive nature of Fondo Riccio eruption compared to Minopoli 1.


*Keywords:* Volcanic risk; Campi Flegrei; Melt inclusions; Volatiles

## 1. Introduction

The geochemical evolution of an active volcanic system and identification of the parameters that play a role in determining the style of an eruption are of fundamental importance to understand the past behavior of a magmatic

* Corresponding author. Virginia Polytechnic Institute & State University, Department of Geosciences, Blacksburg, VA, USA.
*E-mail address:* claudiac@vt.edu (C. Cannatelli).

0009-2541/$ - see front matter © 2006 Elsevier B.V. All rights reserved.
doi:10.1016/j.chemgeo.2006.07.012

system and to forecast future behavior. Development of geochemical models for volcanic eruption forecasting require information on the volatile content of the magma before an eruption, because volatiles play a major role in controlling the nature and style of eruptive events (Anderson, 1976; Burnham, 1979). The exsolution and expansion of volatiles (especially $H_2O$) provides the mechanical energy that drives explosive volcanic eruptions. The original volatile content of magma can be estimated by analyzing melt inclusions (MI) contained in phenocrysts (Anderson, 1974; Clocchiatti, 1975; Roedder, 1979; Belkin et al., 1985; Sobolev et al., 1990; Lowenstern, 1994; Anderson, 2003; Wallace, 2005). Moreover, MI may provide information concerning crystallization and mixing histories of magmas and also the conditions of primary melt generation and extraction (Roedder, 1984; Carroll and Holloway, 1994; Lowenstern, 1994; Sobolev, 1996; Marianelli et al., 1999; Danyushevsky et al., 2000; Frezzotti, 2001).

The Campi Flegrei volcanic complex is an active volcanic field in the Neapolitan area (Italy) that has experienced predominantly explosive volcanic activity for more than 60,000 years. The city of Pozzuoli lies close to the Solfatara crater (actually it was built on the deposits of numerous eruptions of the past 10 ka) while Naples, with 1.5 million inhabitants, is nearby, between Campi Flegrei and Vesuvius. The volcanic risk in this area is significant because of the large population and is a compelling reason to better understand the evolution of the Campi Flegrei complex and the mechanisms that lead to explosive eruptions. We studied the products of two eruptions that occurred in Campi Flegrei during the First Cycle: Fondo Riccio (9.5–10.3 ka) and Minopoli 1 (10.3–11.5 ka). Fondo Riccio was an explosive strombolian eruption that occurred near the center of the Campi Flegrei caldera, whereas Minopoli was an explosive hydromagmatic eruption that occurred along the regional fault system in the northern portion of the Campi Flegrei caldera. Data from MI were used to constrain the evolution of major and volatile ($H_2O$, Cl, S and F) element concentrations, with the goal to reconstruct the crystallization history of the magmas and assess pre-eruptive volatile abundances for the two eruptions.

## 2. Geological setting

The Campi Flegrei Volcanic District lies in the Campanian Plain (CP), between the western side of the Southern Apennine Chain and the eastern border of the Tyrrhenian abyssal plain. Since late Miocene–early Pliocene, the Tyrrhenian Sea has been opening (Scandone, 1979; Doglioni, 1991) and the Calabrian arc has migrated to the SE following rollback of the subducted Ionian plate under Calabria (Selvaggi and Chiarabba, 1995; Piromallo and Morelli, 1997; Gvirtzman and Nur, 2001). Extension in the Tyrrhenian basin was accompanied by contemporaneous compression in the Apennine chain (Meletti et al., 2000). As a result of motions of the Tyrrhenian and Ionian blocks, the CP became a structural depression bordered by NW–SE and NE–SW trending faults (D'Argenio et al., 1973; Ippolito et al., 1975; Hippolyte et al., 1994). Geological, geophysical and petrologic evidence (Selvaggi and Amato, 1992; Serri et al., 1993; Peccerillo, 1999) suggest that subduction of oceanic lithosphere (from the relict Ionian basin) beneath the Apennines occurred concomitant with thinning of the continental lithosphere in the region of the Adriatic Sea, Sicily and North Africa.

The Campi Flegrei caldera (Fig. 1) is one of the most active volcanic systems in the Mediterranean region. The area is known for intense hydrothermal activity, frequent earthquakes and bradyseismic events that occurred between1969–1972 and 1982–1984. The area has been volcanically active for 60 ka (Pappalardo et al., 2002) and many studies have been devoted to understanding its activity (Di Girolamo et al., 1984; Rosi and Sbrana, 1987; Barberi et al., 1991; Pappalardo et al., 1999; De Vivo et al., 2001; Rolandi et al., 2003). At Campi Flegrei, numerous eruptions from multiple sources have produced lava and pyroclastic deposits, including several lava dome structures. Some authors (Rosi and Sbrana, 1987; Orsi et al., 1996) relate the origin of Campi Flegrei either to the eruption of the Campanian Ignimbrite (CI) (39 ka, De Vivo et al., 2001), or to the Neapolitan Yellow Tuff (NYT) (15 ka, Deino et al., 2004). An interpretation that considers the eruption of the CI to be a unique event originating in the Campi Flegrei caldera has been questioned by De Vivo et al. (2001) and Rolandi et al. (2003). These authors describe a sequence of eruptive events from fractures activated along the neotectonic Apennine fault system parallel to the Tyrrhenian coastline. These events, of ignimbritic origin, lasted from >300 ka to 19 ka and are not confined to a unique volcanic center in Campi Flegrei (Rosi and Sbrana, 1987; Orsi et al., 1996). Only the Neapolitan Yellow Tuff (NYT) (15 ka, Deino et al., 2004) erupted within Campi Flegrei, whereas the CI (39 ka, De Vivo et al., 2001) has a much wider source area (Rolandi et al., 2003). According to Pappalardo et al. (2002), the time between the CI and NYT eruptions is characterized by a large number of significantly less powerful events. Volcanism in this interval is poorly defined, primarily because of limited exposure due to cover by younger deposits, restriction to submarine exposure, and intense urbanization. Since the

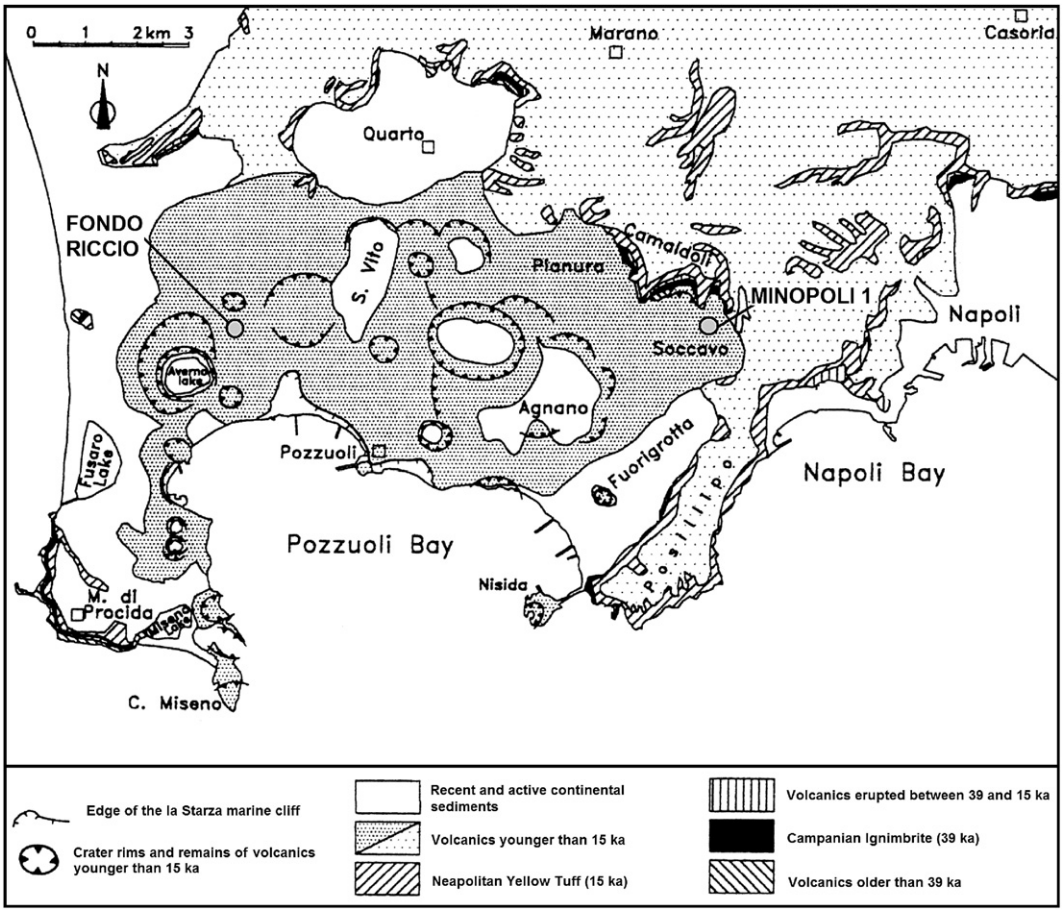


Fig. 1. Schematic map of the Campi Flegrei area showing sample locations (modified after Pappalardo et al., 1999).

NYT eruption the edge of the caldera has been the site of at least 65 eruptions during three periods of activity (15.0–9.5; 8.6–8.2; and 4.8–3.8 ka). These eruptions were separated by quiescent periods marked by two widespread paleosoils (Di Vito et al., 1999). During each eruptive period, eruptions were separated by short-time intervals, on the order of tens of years. The last eruption in 1538 formed the Monte Nuovo cone (Di Vito et al., 1987) after 3.4 ka quiescence.

Campi Flegrei eruptions were mostly explosive with variable degrees of magma/water interaction; only a few events were effusive. The volcanic products range from trachybasalt to alkali-trachyte and phono-trachyte, and are characterized by variable Sr–Nd–Pb–B isotope ratios (D'Antonio et al., 1999; Pappalardo et al., 2002; Tonarini et al., 2004) and involve different magma types (i.e. from different sources and/or with different history) or source processes.

Products from two eruptions that occurred in the First Epoch were studied. The Fondo Riccio eruption occurred at 9.5 ka from an eruptive center on the western side of the Gauro volcano, near the center of the Phlegraean caldera. The eruption was explosive, with strombolian character. The eruptive deposits are composed of coarse scoria beds with subordinate coarse-ash beds and overlay Montagna Spaccata tephra and are in turn overlain by paleosoil A (Di Vito et al., 1999).

The Minopoli 1 eruption was a magmatic eruption, with hydromagmatic phases, that occurred at 11.1 ka, along a regional fault system in the northern sector of the Phlegraean caldera. The eruptive products are composed of alternating pumice lapilli fallout and mainly massive ash fallout, and less abundant cross laminated ash surge beds. The deposits overlay Pomici Principali and are overlain by Montagna Spaccata (Di Vito et al., 1999).

## 3. Samples and methods

Two samples were collected from each unit. Sample CF-FR-C1 is a scoria and sample CF-FR-C2 is a lava bomb from the Fondo Riccio unit. Both samples are porphyritic latite, with abundant crystals in a glassy,

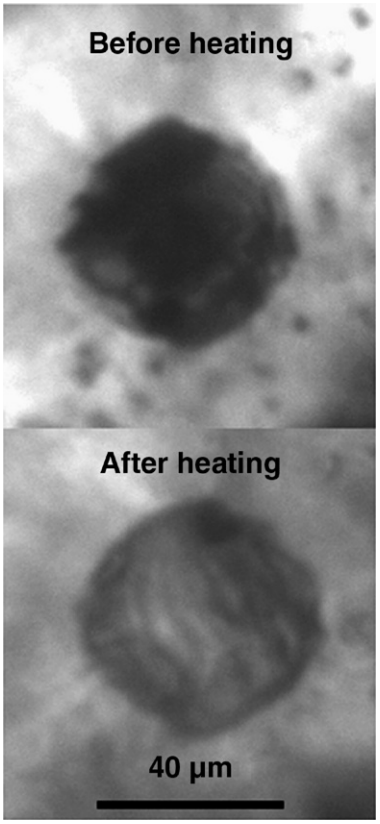


Fig. 2. Change in appearance of two crystallized silicate melt inclusions hosted in clinopyroxene in Fondo Riccio scoria as a result of heating from room temperature (22 °C) to the homogenization temperature (1137 °C). After heating to 1137 °C the inclusion contains only a vapor bubble. The MI is approximately 40 μm in diameter.

vesicular groundmass, and were deposited between 9.5 and 10.3 ka (Di Vito et al., 1999). The bulk rock contains less than 10% phenocrysts, which include clinopyroxene, olivine and biotite with subordinate plagioclase and magnetite. In thin section clinopyroxene and plagioclase are found in small clots; these minerals also occur among microlites. Silicate MIs in olivine and pyroxene phenocrysts from sample FR-C1 and in clinopyroxenes for the sample FR-C2 were studied. For the Minopoli 1 unit, sample MI1-C1 is a scoria and sample MI1-C2 is a cohesive scoria sampled along the caldera rim, and was likely erupted during the final magmatic stage of the eruption. The deposits include scoria and ash layers. Both samples are porphyritic trachybasalt and range from 11.1 and 10.3 ka (Di Vito et al., 1999). The bulk rock contains about 20% phenocrysts, which include clinopyroxene, olivine and biotite. Silicate MI in olivine and pyroxene from Mi1-C1 and in clinopyroxene from MI1-C2 were studied.

The abundance of MI varies from crystal to crystal in the same sample. Melt inclusions consist of silicate glass, generally devitrified, with a shrinkage bubble and daughter crystals (usually apatite or Fe/Ti oxides). MIs generally have elongated rectangular shapes and range from 30 to 80 μm (most between 20 and 50 μm) (Fig. 2). Rock samples were hand crushed and phenocrysts were hand picked, mounted on a glass slide, and doubly polished to improve the optical clarity during microscope heating experiments.

MI from Fondo Riccio and Minopoli 1 were partially or totally recrystallized when found and required heating and quenching to obtain a homogeneous glass. Heating experiments have been carried out at the Department of Geosciences at Virginia Tech (Blacksburg, USA) using the heating stage designed and built at the Vernadsky Institute, Moscow (Sobolev and Slutskii, 1984). All the experiments were conducted in controlled (inert gas) atmosphere to avoid oxidation of the crystal

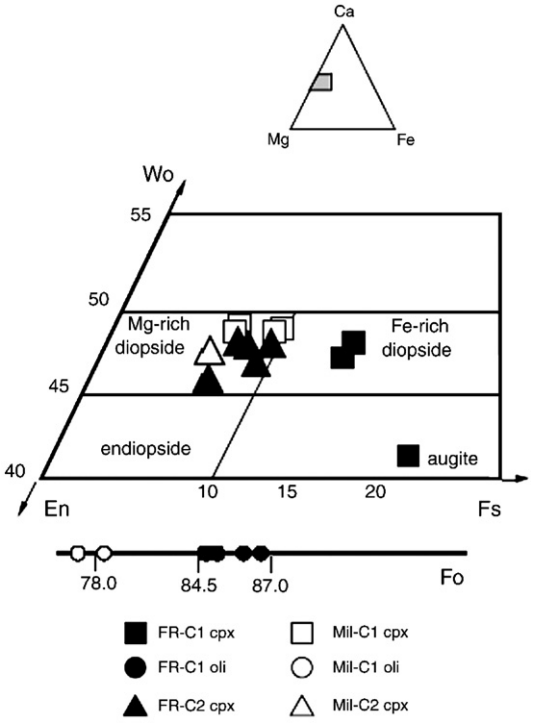


Fig. 3. Classification diagrams for pyroxene and olivine phenocrysts (Morimoto, 1988). Filled squares = compositions of MI hosted in clinopyroxene from FR-C1 (scoria); filled circles = composition of MI hosted in olivine from FR-C1 (scoria); filled triangles = compositions of MI hosted in clinopyroxene from FR-C2 (bomb); open squares = compositions of MI hosted in clinopyroxene from Mi1-C1; open circles = compositions of MI hosted in olivine from Mi1-C1; open triangles = composition of MI hosted in clinopyroxenes from Mi1-C2.

Table 1a
MI composition from Fondo Riccio C1 sample determined by EMPA and SIMS. T(quen)=maximum temperature of heating experiment; Cpx=clinopyroxene host crystal; Ol=olivine host crystal

| Sample | FR-C1 | FR-C1 | FR-C1 | FR-C1 | FR-C1 | FR-C1 | FR-C1 | FR-C1 | FR-C1 | FR-C1 | FR-C1 | FR-C1 | FR-C1 | FR-C1 | FR-C1 |
|---|---|---|---|---|---|---|---|---|---|---|---|---|---|---|---|
| Label MI | p6 M1 | p6 M2 | p6 M4 | p6 M5 | p6 M6 | p6 M7 | p6 M8 | p6 M9 | p11 M1 | p12 M1 | p12 M2 | o1 M1 | o2 M1 | o4 M1 | o6 M1 |
| Size (μm) | 75 | 80 | 35 | 30 | 60 | 55 | 75 | 55 | 85 | 50 | 130 | 70 | 50 | 60 | 50 |
| Host xl | Cpx | Cpx | Cpx | Cpx | Cpx | Cpx | Cpx | Cpx | Cpx | Cpx | Cpx | Ol | Ol | Ol | Ol |
| *T* (quen) °C | 1126 | 1126 | 1126 | 1126 | 1126 | 1126 | 1126 | 1126 | 1145 | 1139 | 1139 | 1172 | 1150 | 1175 | 1135 |
| Host Mg# | 74.41 | 73.37 | 73.68 | 75.16 | 76.11 | 83.17 | 78.04 | 86.12 | 83.17 | 78.04 | 86.12 | 86.77 | 86.56 | 84.95 | 84.70 |
| *Host xl composition* | | | | | | | | | | | | | | | |
| °C | | | | | | | | | | | | | | | |
| $SiO_2$ | 49.93 | 50.24 | 50.24 | 50.36 | 50.36 | 50.36 | 50.74 | 50.41 | 51.68 | 49.01 | 49.80 | 40.15 | 40.02 | 40.74 | 39.77 |
| $TiO_2$ | 0.62 | 0.63 | 0.63 | 0.63 | 0.63 | 0.63 | 0.59 | 0.53 | 0.32 | 0.77 | 0.67 | 0.05 | 0.00 | 0.04 | 0.00 |
| $Al_2O_3$ | 3.21 | 3.35 | 3.35 | 3.02 | 3.02 | 3.02 | 3.27 | 3.17 | 3.02 | 4.13 | 3.63 | 0.01 | 0.01 | 0.03 | 0.02 |
| FeO | 8.52 | 8.71 | 8.71 | 8.71 | 8.71 | 8.71 | 8.17 | 7.99 | 5.62 | 7.43 | 6.49 | 13.06 | 12.90 | 13.89 | 14.71 |
| MnO | 0.44 | 0.48 | 0.48 | 0.40 | 0.40 | 0.40 | 0.39 | 0.39 | 0.11 | 0.24 | 0.21 | 0.23 | 0.25 | 0.28 | 0.30 |
| MgO | 13.90 | 13.47 | 13.47 | 13.68 | 13.68 | 13.68 | 13.87 | 14.27 | 15.59 | 14.83 | 15.23 | 48.06 | 46.62 | 44.00 | 45.71 |
| CaO | 22.45 | 22.41 | 22.41 | 22.25 | 22.25 | 22.25 | 22.04 | 21.92 | 22.78 | 21.91 | 22.37 | 0.36 | 0.32 | 0.30 | 0.31 |
| $Na_2O$ | 0.36 | 0.41 | 0.41 | 0.37 | 0.37 | 0.37 | 0.34 | 0.37 | 0.17 | 0.28 | 0.22 | 0.03 | 0.01 | 0.01 | 0.01 |
| $K_2O$ | 0.02 | 0.00 | 0.00 | 0.02 | 0.02 | 0.02 | 0.01 | 0.00 | 0.01 | 0.01 | 0.02 | 0.02 | 0.01 | 0.00 | 0.03 |
| $P_2O_5$ | 0.02 | 0.02 | 0.02 | 0.02 | 0.02 | 0.02 | 0.03 | 0.00 | 0.01 | 0.01 | 0.01 | 0.02 | 0.01 | 0.00 | 0.02 |
| Total | 99.57 | 99.99 | 99.99 | 99.67 | 99.67 | 99.67 | 99.50 | 99.09 | 99.36 | 98.71 | 98.70 | 102.14 | 98.82 | 99.38 | 100.90 |
| Wo | 27.3 | 27.3 | 27.3 | 27.3 | 27.3 | 27.3 | 27.3 | 27.3 | 51.7 | 50.5 | 50.5 | 0.6 | 0.5 | 0.5 | 0.5 |
| En | 56.5 | 56.5 | 56.5 | 56.5 | 56.5 | 56.5 | 56.5 | 56.5 | 35.4 | 34.4 | 34.4 | 77.9 | 77.6 | 75.3 | 74.9 |
| Fs | 16.2 | 16.2 | 16.2 | 16.2 | 16.2 | 16.2 | 16.2 | 16.2 | 13.0 | 15.1 | 15.1 | 21.5 | 21.9 | 24.2 | 24.6 |
| Melt inclusion composition | | | | | | | | | | | | | | | |
| *Electron microprobe* | | | | | | | | | | | | | | | |
| $SiO_2$ | 57.86 | 58.12 | 58.18 | 58.80 | 58.16 | 58.30 | 59.38 | 56.06 | 52.06 | 55.06 | 48.33 | 47.69 | 46.83 | 48.09 | 49.57 |
| $TiO_2$ | 0.53 | 0.54 | 0.48 | 0.51 | 0.53 | 0.46 | 0.47 | 0.61 | 0.72 | 0.66 | 0.98 | 0.87 | 0.89 | 0.94 | 0.87 |
| $Al_2O_3$ | 16.32 | 16.61 | 17.55 | 16.35 | 17.33 | 16.56 | 18.32 | 17.44 | 18.88 | 18.19 | 14.39 | 13.88 | 12.77 | 14.31 | 16.52 |
| $FeO^{tot}$ | 4.01 | 3.58 | 2.77 | 3.54 | 2.97 | 3.61 | 1.98 | 5.21 | 4.68 | 3.51 | 5.94 | 7.21 | 8.22 | 7.71 | 6.86 |
| MnO | 0.26 | 0.23 | 0.16 | 0.32 | 0.14 | 0.16 | 0.13 | 0.07 | 0.15 | 0.06 | 0.11 | 0.12 | 0.18 | 0.17 | 0.18 |
| MgO | 1.91 | 1.74 | 1.44 | 1.64 | 1.47 | 1.66 | 1.21 | 2.05 | 3.08 | 2.25 | 6.11 | 8.05 | 9.45 | 6.92 | 4.91 |
| CaO | 4.81 | 4.74 | 4.14 | 4.54 | 4.16 | 4.51 | 3.66 | 5.02 | 7.32 | 7.42 | 11.35 | 10.15 | 9.42 | 9.96 | 9.86 |
| $Na_2O$ | 3.40 | 3.61 | 3.60 | 3.38 | 3.73 | 3.53 | 3.57 | 3.60 | 3.70 | 2.54 | 1.73 | 1.57 | 1.33 | 1.41 | 1.72 |
| $K_2O$ | 7.65 | 7.78 | 8.18 | 7.69 | 8.25 | 7.94 | 8.57 | 7.12 | 5.42 | 6.92 | 4.64 | 4.67 | 4.41 | 4.58 | 5.21 |
| $P_2O_5$ | 0.22 | 0.14 | 0.27 | 0.14 | 0.21 | 0.14 | 0.27 | 0.30 | 1.03 | 0.31 | 0.87 | 0.61 | 0.62 | 0.56 | 0.67 |
| NiO | 0.00 | 0.00 | 0.00 | 0.00 | 0.00 | 0.00 | 0.00 | 0.00 | 0.00 | 0.00 | 0.00 | 0.00 | 0.00 | 0.00 | 0.00 |
| $SO_2$ | 0.07 | 0.06 | 0.04 | 0.13 | 0.08 | 0.07 | 0.09 | 0.04 | 0.16 | 0.05 | 0.29 | 0.33 | 0.40 | 0.31 | 0.25 |
| F | 0.21 | 0.12 | 0.14 | 0.17 | 0.17 | 0.22 | 0.28 | 0.17 | 0.31 | 0.00 | 0.08 | 0.27 | 0.14 | 0.15 | 0.18 |
| Cl | 0.58 | 0.71 | 0.57 | 0.56 | 0.54 | 0.62 | 0.53 | 0.46 | 0.58 | 0.32 | 0.47 | 0.42 | 0.44 | 0.47 | 0.42 |
| Total | 97.83 | 97.96 | 97.52 | 97.76 | 97.74 | 97.76 | 98.46 | 98.15 | 98.09 | 97.27 | 95.29 | 95.85 | 95.08 | 95.58 | 97.22 |
| *Ion microprobe* | | | | | | | | | | | | | | | |
| $H_2O$ (wt.%) | – | 6.96 | – | – | – | – | 3.66 | – | – | – | – | 4.13 | – | 3.61 | – |
| Li | – | 28 | – | – | – | – | 26 | – | – | – | – | 15 | – | 11 | – |
| Be | – | 13 | – | – | – | – | 16 | – | – | – | – | 9 | – | 52 | – |
| B | – | 62 | – | – | – | – | 59 | – | – | – | – | 39 | – | 55 | – |
| Rb | – | 316 | – | – | – | – | 316 | – | – | – | – | 218 | – | 276 | – |
| Sr | – | 627 | – | – | – | – | 614 | – | – | – | – | 1043 | – | 902 | – |
| Y | – | 53 | – | – | – | – | 35 | – | – | – | – | 45 | – | 43 | – |
| Zr | – | 384 | – | – | – | – | 262 | – | – | – | – | 176 | – | 292 | – |
| Nb | – | 49 | – | – | – | – | 48 | – | – | – | – | 23 | – | 35 | – |
| Cs | – | 25 | – | – | – | – | 16 | – | – | – | – | 19 | – | 19 | – |
| Ce | – | 172 | – | – | – | – | 128 | – | – | – | – | 112 | – | 98 | – |
| Nd | – | 47 | – | – | – | – | 32 | – | – | – | – | 38 | – | 97 | – |
| Sm | – | 1 | – | – | – | – | 1 | – | – | – | – | 2 | – | 3 | – |
| Dy | – | 4 | – | – | – | – | <1 | – | – | – | – | 2 | – | 3 | – |

Table 1a (*continued*)

| Sample | FR-C1 | FR-C1 | FR-C1 | FR-C1 | FR-C1 | FR-C1 | FR-C1 | FR-C1 | FR-C1 | FR-C1 | FR-C1 | FR-C1 | FR-C1 | FR-C1 | FR-C1 |
|---|---|---|---|---|---|---|---|---|---|---|---|---|---|---|---|
| Label MI | p6 M1 | p6 M2 | p6 M4 | p6 M5 | p6 M6 | p6 M7 | p6 M8 | p6 M9 | p11 M1 | p12 M1 | p12 M2 | o1 M1 | o2 M1 | o4 M1 | o6 M1 |
| *Ion microprobe* | | | | | | | | | | | | | | | |
| Yb | – | 1 | – | – | – | – | <1 | – | – | – | – | 2 | – | 2 | – |
| Th | – | 29 | – | – | – | – | 25 | – | – | – | – | 21 | – | 19 | – |
| U | – | 12 | – | – | – | – | 7 | – | – | – | – | 5 | – | 9 | – |

according to the procedure described in Danyushevsky et al. (2000) and Lima (2000). The precision of temperature measurements is ±3 °C at 1200 °C (measured by thermocouple), based on calibration using known melting points of Ag (938 °C) and Au (1064 °C). The inclusions were heated until all solid phases disappeared. Total homogenization (i.e. disappearance of the bubble) was not attempted to avoid decrepitation. The partial homogenization temperature ($T_h$) thus represents a minimum estimate of the trapping temperature.

After quenching, single crystals were mounted with epoxy on transparent polycarbonate rods and polished according to the technique described by Thomas and Bodnar (2002) to expose MI. MI were analyzed with a Cameca SX/50 Microprobe at University of Rome "La Sapienza" (IGAG-CNR, Rome, Italy) and at Virginia Tech (Blacksburg, USA). Analyses were performed at 15 kV, using a current of 10 nA with a defocused beam diameter of 10 μm and counting time of 10 s, as recommended by Morgan and London (1996). Relative one-sigma precision is estimated to be 1 to 2% for major elements and 5 to 10% for minor elements. In each analytical run, alkalis were counted first, and no correction has been made for Na loss. Test runs made prior to the beginning of the analysis on synthetic and natural glass standards of known composition showed no significant alkali migration under the specified analytical conditions. Two points were analyzed in larger MI, whereas only one point was analyzed in smaller inclusions (<10 μm). When no significant difference in composition was detected, an average of the two analyses was used. If the two analyses were significantly different the results were discarded. If just one spot was possible, a comparison between the obtained data and data for other MI in the same sample was made to test for consistency. Note, however, that two or more analyses were obtained on ~90% of the MI. Host phenocrysts were analyzed at distances of about 20 μm from MI with accelerating voltage of 15 kV and beam current of 10 nA.

Selected MI were analyzed for H (reported as $H_2O$), Li, Be, B, Rb, Sr, Y, Zr, Nb, Cs, Ce, Sm, Dm, Yb, Th and U by Secondary Ion mass Spectrometry (SIMS) at the Woods Hole Oceanographic Institution, using techniques detailed by Shimizu and Hart (1982) and Webster et al. (1996). Accelerating potential was 10 kV and beam current was 1–2 nA. The inclusions were analyzed in one spot, five times each in depth profile mode. Precision and accuracy were monitored with NBS (National Bureau of Standards) reference glasses NBS 610. Results on the NBS glasses are similar and within 5% of the accepted values; $H_2O$ concentrations are reproducible to +0.3 to 0.4 wt.% and trace elements to 5 to 15% (for more details see Webster et al., 2001).

## 4. Results and discussion

Fondo Riccio olivine compositions range from $Fo_{84}$ to $Fo_{87}$, while Minopoli 1 olivines range from $Fo_{77}$ to $Fo_{78}$ (Fig. 3). Clinopyroxene compositions fall in the diopside–salite field ($Wo_{44-48}$, $Fs_{5-19}$) and Mg # (calculated based on total Fe) varies from about 73.4 to 88.6 for Fondo Riccio samples (with a compositional gap between 78 and 83) and from about 85.1 to 89.9 for Minopoli 1 samples. Clinopyroxenes are low-Ti, which is a characteristic of "HKS"-type lavas of the Roman Comagmatic Province (Cundari and Fergusson, 1982).

Homogenization temperatures of MI in clinopyroxene and olivine from the scoria of Fondo Riccio (FR-C1) average 1135±3 °C and 1155±3 °C, respectively, whereas MI in clinopyroxene from the bomb sample (FR-C2) average 1159±3 °C. Homogenization temperatures of Minopoli 1 MI in clinopyroxenes average 1132±3 °C and those in olivine average 1145±3 °C.

The maximum temperature achieved during heating experiments does not equal the trapping temperature because a bubble still remained in the inclusions. MI compositions can be depleted in the host mineral components if the maximum temperature of heating is below the trapping temperature. Thus, the concentrations of most elements in the quenched MI may not reflect their original values in the trapped melt. However, ratios of elements that are incompatible in the host, and also concentrations of elements that are present at similar levels in the melt and the host, should not be significantly affected by over- or under-heating. Moreover, Fedele et al. (2003) have shown that compositions of MI

obtained from inclusions that were heated until all of the solids had melted (with the bubble still present) and quenched were in good agreement with melt compositions predicted by the MELTS program (see also Thomas et al., 2002).

Representative compositions of MI (average values) hosted in Fondo Riccio clinopyroxene and olivine are shown together with MI size, maximum temperature ($T_{run}$) and host crystal Mg# in Table 1a (FR-C1) and 1b (FR-C2). Representative compositions of MI from Minopoli 1 are shown in Table 1c. All MIs are characterized by analytical totals <100. This is interpreted to reflect the presence of $H_2O$ in the MI, as confirmed by secondary ion mass spectrometry (SIMS) analyses that show average $H_2O$ contents between 3.3–6.9 wt.% for Fondo Riccio samples and between 1.3–5.2 wt.% for Minopoli 1 samples (Tables 1a–c).

MIs from Fondo Riccio show a broad range for $SiO_2$ (46.8–59.3 wt.%), CaO (3.66–12.4 wt.%), $Na_2O$ (1.3–3.7 wt.%) and $K_2O+Na_2O$ (4.19–9.73 wt.%). Conversely, MI from Minopoli 1 show narrow ranges for $SiO_2$ (49.6–51.8 wt.%), CaO (7.6–13.3 wt.%), $Na_2O$ (1.0–1.8 wt.%) and $K_2O+Na_2O$ (4.19–9.73 wt.%) as shown in Tables 1a–c.

On the total alkali-$SiO_2$ classification diagram (Fig. 4; Le Bas et al., 1986) the Fondo Riccio bulk-rock composition is in the latite field. Fondo Riccio MI data show two trends: from latite to trachyte for MI in Fe-rich diopside (sample CF-FR-C1) and from trachybasalt to shoshonite for MI in both Mg-rich diopside (sample CF-FR-C2) and olivine (sample CF-FR-C1). The Minopoli 1 bulk-rock composition is in the trachyandesite field, whereas MI data show two different compositions: basalt for MI in clinopyroxenes from the lower unit (Mi1-C1) and trachybasalt for MI in olivine (Mi1-C1) and clinopyroxenes from the upper unit (Mi1-C2). Except for clinopyroxene in FR-C1, MIs are generally less evolved than the corresponding host rock. In particular, MIs in olivine from CF-FR-C1 scoria show the same, less evolved composition as MI in clinopyroxene from CF-FR-C2 bomb sample. The Fondo Riccio bulk rock is depleted in $K_2O$ (not shown in the variation diagrams) and enriched in $TiO_2$ and $Na_2O$ compared with MI with similar Mg# hosted in clinopyroxene from the CF-FR-C1 scoria sample. Harker diagrams showing major element concentrations of MI as a function of $SiO_2$ show a wider range in composition in Fondo Riccio samples than Minopoli 1 (Fig. 5). MI in clinopyroxene and olivine from both samples show decreasing $Al_2O_3$ (Fig. 5a) and $Na_2O$ (Fig. 5f) and increasing $FeO^{tot}$ (Fig. 5b), $TiO_2$ (Fig. 5c), MgO (Fig. 5d) and CaO (Fig. 5e) with decreasing $SiO_2$.

Table 1b
MI composition of Fondo Riccio C2 sample determined by EMPA and SIMS

| Sample | FR-C2 | FR-C2 | FR-C2 | FR-C2 | FR-C2 |
|---|---|---|---|---|---|
| Label MI | p2 M1 | p4 M1 | p5 M1 | p6 M1 | p7 M1 |
| Size (μm) | 20 | 40 | 80 | 100 | 40 |
| Host xl | Cpx | Cpx | Cpx | Cpx | Cpx |
| *T* (quen)°C | 1176 | 1135 | 1165 | 1152 | 1164 |
| Host Mg# | 88.68 | 86.94 | 88.57 | 84.98 | 84.62 |
| *Host xl composition* | | | | | |
| $SiO_2$ | 53.70 | 52.03 | 52.11 | 51.25 | 51.67 |
| $TiO_2$ | 0.36 | 0.44 | 0.39 | 0.60 | 0.54 |
| $Al_2O_3$ | 2.09 | 2.48 | 2.11 | 2.79 | 3.21 |
| FeO | 3.76 | 4.38 | 3.93 | 5.06 | 5.00 |
| MnO | 0.10 | 0.14 | 0.08 | 0.17 | 0.12 |
| MgO | 16.53 | 16.36 | 17.09 | 16.07 | 15.44 |
| CaO | 23.25 | 23.01 | 23.00 | 22.47 | 23.02 |
| $Na_2O$ | 0.11 | 0.11 | 0.09 | 0.15 | 0.12 |
| $K_2O$ | 0.00 | 0.01 | 0.02 | 0.01 | 0.00 |
| $P_2O_5$ | 0.02 | 0.04 | 0.01 | 0.06 | 0.01 |
| Total | 100.07 | 99.05 | 98.94 | 98.67 | 99.20 |
| Wo | 53.3 | 52.4 | 52.2 | 51.3 | 52.8 |
| En | 37.9 | 37.3 | 38.8 | 36.7 | 35.4 |
| Fs | 8.8 | 10.3 | 9.1 | 11.9 | 11.7 |
| Melt inclusion composition | | | | | |
| *Electron microprobe* | | | | | |
| $SiO_2$ | 49.09 | 49.08 | 48.87 | 47.72 | 53.01 |
| $TiO_2$ | 1.00 | 0.97 | 0.91 | 1.28 | 1.06 |
| $Al_2O_3$ | 12.84 | 13.86 | 12.76 | 12.81 | 20.34 |
| $FeO^{tot}$ | 7.00 | 5.94 | 6.57 | 7.92 | 3.44 |
| MnO | 0.10 | 0.15 | 0.15 | 0.28 | 0.16 |
| MgO | 6.81 | 6.17 | 7.33 | 6.90 | 2.12 |
| CaO | 10.65 | 11.27 | 11.88 | 12.40 | 6.06 |
| $Na_2O$ | 1.31 | 1.42 | 1.46 | 1.36 | 2.83 |
| $K_2O$ | 4.07 | 4.20 | 4.23 | 2.60 | 7.83 |
| $P_2O_5$ | 0.60 | 0.36 | 0.44 | 0.46 | 1.36 |
| NiO | 0.00 | 0.00 | 0.00 | 0.00 | 0.00 |
| $SO_2$ | 0.34 | 0.27 | 0.19 | 0.26 | 0.13 |
| F | 0.07 | 0.40 | 0.18 | 0.10 | 0.08 |
| Cl | 0.44 | 0.40 | 0.43 | 0.33 | 0.39 |
| Total | 94.31 | 94.49 | 95.40 | 94.42 | 98.81 |
| *Ion microprobe* | | | | | |
| $H_2O$ (wt.%) | 3.25 | – | – | – | – |
| Li (ppm) | 11 | – | – | – | – |
| Be (ppm) | 3 | – | – | – | – |
| B (ppm) | 24 | – | – | – | – |
| Rb | 98 | – | – | – | – |
| Sr | 431 | – | – | – | – |
| Y | 25 | – | – | – | – |
| Zr | 136 | – | – | – | – |
| Nb | 16 | – | – | – | – |
| Cs | 15 | – | – | – | – |
| Ce | 48 | – | – | – | – |
| Nd (ppm) | 16 | – | – | – | – |
| Sm (ppm) | 3 | – | – | – | – |
| Dy | 1 | – | – | – | – |
| Yb | 1 | – | – | – | – |
| Th | 7 | – | – | – | – |
| U | 6 | – | – | – | – |

Table 1c
MI composition of Minopoli 1 sample determined by EMPA and SIMS

| Sample | Mi 1-C1 | Mi 1-C1 | Mi 1-C1 | Mi 1-C1 | Mi 1-C1 | Mi 1-C1 | Mi 1-C1 | Mi 1-C2 | Mi 1-C2 |
|---|---|---|---|---|---|---|---|---|---|
| Label MI | p2 M1 | p3 M1 | p6 M1 | p6 M2 | p8 M1 | o5 M1 | o6 M1 | p1 M1 | p1 M2 |
| Size (μm) | 50 | 60 | 50 | 70 | 40 | 60 | 55 | 45 | 50 |
| Host xl | Cpx | Cpx | Cpx | Cpx | Cpx | Olivine | Olivine | Cpx | Cpx |
| *T* (quen) °C | 1122 | 1149 | 1156 | 1156 | 1108 | 1120 | 1145 | 1122 | 1122 |
| Host Mg# | 86.64 | 88.59 | 85.10 | 86.10 | 86.29 | 86.68 | 85.68 | 89.89 | 89.89 |
| *Host xl composition* | | | | | | | | | |
| $SiO_2$ | 52.39 | 52.96 | 52.52 | 52.52 | 52.78 | 39.38 | 38.96 | 52.67 | 52.67 |
| $TiO_2$ | 0.41 | 0.33 | 0.43 | 0.43 | 0.36 | 0.00 | 0.01 | 0.25 | 0.25 |
| $Al_2O_3$ | 3.03 | 2.19 | 3.35 | 3.35 | 2.78 | 0.02 | 0.02 | 1.68 | 1.68 |
| FeO | 4.36 | 3.72 | 4.97 | 4.97 | 4.58 | 12.66 | 13.70 | 3.37 | 3.37 |
| MnO | 0.14 | 0.10 | 0.10 | 0.10 | 0.11 | 0.20 | 0.22 | 0.09 | 0.09 |
| MgO | 15.86 | 16.20 | 15.92 | 15.92 | 16.18 | 46.22 | 45.99 | 16.82 | 16.82 |
| CaO | 22.75 | 23.39 | 21.52 | 21.52 | 22.53 | 0.28 | 0.27 | 23.53 | 23.53 |
| $Na_2O$ | 0.14 | 0.13 | 0.15 | 0.15 | 0.13 | 0.02 | 0.04 | 0.15 | 0.15 |
| $K_2O$ | 0.01 | 0.03 | 0.02 | 0.02 | 0.01 | 0.03 | 0.01 | 0.01 | 0.01 |
| $P_2O_5$ | 0.02 | 0.04 | 0.00 | 0.00 | 0.00 | 0.00 | 0.02 | 0.00 | 0.00 |
| Total | 99.11 | 99.07 | 98.99 | 98.99 | 99.45 | 98.82 | 99.22 | 98.56 | 98.56 |
| Wo | 52.8 | 53.9 | 50.6 | 50.6 | 51.9 | 0.5 | 0.4 | 53.7 | 53.7 |
| En | 36.8 | 37.3 | 37.5 | 37.5 | 37.3 | 77.9 | 76.4 | 38.4 | 38.4 |
| Fs | 10.4 | 8.8 | 11.9 | 11.9 | 10.8 | 21.7 | 23.1 | 7.9 | 7.9 |
| Melt inclusion composition | | | | | | | | | |
| *Electron microprobe* | | | | | | | | | |
| $SiO_2$ | 46.94 | 48.20 | 51.79 | 49.96 | 50.19 | 47.81 | 47.96 | 51.11 | 50.75 |
| $TiO_2$ | 1.05 | 0.76 | 0.68 | 0.76 | 0.79 | 0.66 | 0.78 | 0.72 | 0.90 |
| $Al_2O_3$ | 13.97 | 11.98 | 10.70 | 10.15 | 16.54 | 13.81 | 14.61 | 13.18 | 13.47 |
| $FeO^{tot}$ | 9.58 | 8.20 | 7.50 | 7.66 | 5.99 | 6.80 | 7.73 | 6.84 | 7.11 |
| MnO | 0.29 | 0.10 | 0.21 | 0.15 | 0.17 | 0.12 | 0.08 | 0.10 | 0.17 |
| MgO | 5.65 | 8.00 | 7.98 | 8.93 | 5.40 | 11.53 | 9.37 | 6.92 | 6.93 |
| CaO | 10.80 | 12.75 | 12.23 | 13.35 | 9.20 | 7.57 | 8.94 | 10.34 | 11.01 |
| $Na_2O$ | 1.82 | 1.30 | 1.16 | 1.03 | 1.71 | 1.50 | 1.57 | 1.24 | 1.30 |
| $K_2O$ | 3.24 | 3.17 | 2.91 | 2.58 | 4.76 | 4.11 | 3.92 | 3.88 | 4.07 |
| $P_2O_5$ | 0.38 | 0.38 | 0.26 | 0.24 | 0.70 | 0.98 | 0.56 | 0.64 | 0.62 |
| NiO | 0.14 | 0.05 | 0.04 | 0.00 | 0.02 | 0.08 | 0.05 | 0.00 | 0.00 |
| $SO_2$ | 0.11 | 0.91 | 0.09 | 0.10 | 0.10 | 0.34 | 0.21 | 0.31 | 0.37 |
| F | 0.29 | 0.03 | 0.01 | 0.03 | 0.09 | 0.07 | 0.17 | 0.00 | 0.00 |
| Cl | 0.30 | 0.28 | 0.20 | 0.20 | 0.34 | 0.43 | 0.43 | 0.42 | 0.39 |
| Total | 94.56 | 96.11 | 95.74 | 95.14 | 96.00 | 95.81 | 96.38 | 95.68 | 97.06 |
| *Ion microprobe* | | | | | | | | | |
| $H_2O$ (wt.%) | 5.15 | – | 1.93 | 1.29 | 5.28 | 3.89 | 4.40 | 5.15 | – |
| Li | 21 | – | 11 | 12 | 24 | 7 | 18 | 21 | – |
| Be | 14 | – | 7 | 77 | 7 | 12 | 1 | 14 | – |
| B | 31 | – | 27 | 320 | 44 | 36 | 32 | 47 | – |
| Rb | 97 | – | 324 | 122 | 215 | 168 | 167 | 176 | – |
| Sr | 667 | – | 614 | 480 | 765 | 607 | 889 | 646 | – |
| Y | 92 | – | 52 | 63 | 37 | 27 | 42 | 37 | – |
| Zr | 266 | – | 262 | 160 | 162 | 437 | 116 | 139 | – |
| Nb | 14 | – | 48 | 14 | 23 | 19 | 16 | 22 | – |
| Cs | 6 | – | 16 | 4 | 16 | 10 | 8 | 93 | – |
| Ce | 180 | – | 128 | 83 | 88 | 69 | 87 | 79 | – |
| Nd | 180 | – | 32 | 74 | 63 | 61 | 75 | 53 | – |
| Sm | 4 | – | 1 | 2 | 2 | 1 | 1 | 1 | – |
| Dy | 2 | – | <1 | 1 | 1 | <1 | <1 | <1 | – |
| Yb | <1 | – | 1 | <1 | 1 | <1 | <1 | <1 | – |
| Th | 5 | – | 25 | 3 | 14 | 9 | 6 | 13 | – |
| U | 1 | – | 7 | 2 | 4 | 3 | 1 | <1 | – |

Table 2
Fondo Riccio and Minopoli 1 bulk rock compositions determined by XRF

| | | CF-FR-C1 | RE CF-FR-C1 | CF-FR-C2 | CF-MI1-C1 | CF-MI1-C2 |
|---|---|---|---|---|---|---|
| $SiO_2$ | wt.% | 54.76 | 54.68 | 54.10 | 52.76 | 57.40 |
| $Al_2O_3$ | wt.% | 17.99 | 18.11 | 17.98 | 17.32 | 17.97 |
| $Fe_2O_3$ | wt.% | 7.26 | 7.23 | 7.61 | 7.44 | 4.87 |
| MgO | wt.% | 2.33 | 2.31 | 2.53 | 3.53 | 1.26 |
| CaO | wt.% | 5.62 | 5.64 | 5.97 | 7.79 | 3.94 |
| NaO | wt.% | 4.49 | 4.59 | 4.46 | 3.05 | 3.52 |
| $K_2O$ | wt.% | 4.35 | 4.34 | 4.35 | 4.79 | 7.94 |
| $TiO_2$ | wt.% | 0.82 | 0.82 | 0.86 | 0.87 | 0.53 |
| $P_2O_5$ | wt.% | 0.52 | 0.51 | 0.58 | 0.58 | 0.23 |
| MnO | wt.% | 0.13 | 0.13 | 0.13 | 0.12 | 0.12 |
| $Cr_2O_3$ | wt.% | 0.03 | 0.03 | 0.01 | 0.01 | 0.02 |
| Ni | ppm | 12.00 | 13.00 | 6.00 | 19.00 | 6.00 |
| Sc | ppm | 10.00 | 10.00 | 11.00 | 15.00 | 5.00 |
| LOI | wt.% | 1.20 | 1.10 | 0.90 | 1.30 | 1.80 |
| Tot/C | wt.% | 0.01 | 0.01 | 0.01 | 0.05 | 0.03 |
| Tot/S | wt.% | 0.01 | 0.01 | 0.01 | 0.01 | 0.05 |
| Sum | wt.% | 99.50 | 99.49 | 99.48 | 99.56 | 99.59 |
| FeO* | wt.% | 3.2 | 3.2 | 4.05 | 4.17 | 2.39 |
| Mo | ppm | 2.40 | 2.5 | 2 | 1.6 | 0.5 |
| Cu | ppm | 7.40 | 6.6 | 7.5 | 15.3 | 3.8 |
| Pb | ppm | 6.50 | 6.3 | 7.2 | 10.8 | 3.9 |
| Zn | ppm | 62.00 | 60 | 73 | 44 | 9 |
| Ni | ppm | 5.30 | 5 | 3 | 7.6 | 2.9 |
| As | ppm | 4.70 | 4.8 | 5.7 | 3.8 | 1.9 |
| Cd | ppm | <.1 | <.1 | <.1 | 0.1 | <.1 |
| Sb | ppm | 0.20 | 0.2 | 0.2 | 0.1 | 0.1 |
| Bi | ppm | 0.10 | 0.1 | <.1 | 0.1 | 0.1 |
| Ag | ppm | <.1 | <.1 | <.1 | <.1 | <.1 |
| Au | ppm | 1.00 | <.5 | 2.4 | 1.6 | 2.5 |
| Hg | ppm | <.01 | <.01 | 0.01 | 0.01 | <.01 |
| Tl | ppm | 0.50 | 0.5 | 0.2 | 0.5 | 0.1 |
| Se | ppm | <.5 | <.5 | <.5 | <.5 | <.5 |
| Ba | ppm | 1719.20 | 1654 | 1712.1 | 1715.2 | 1048.9 |
| Be | ppm | 7.00 | 9 | 7 | 7 | 10 |
| Co | ppm | 15.90 | 16.4 | 17.2 | 21.5 | 7.6 |
| Cs | ppm | 16.90 | 16.7 | 16.2 | 11.8 | 16.1 |
| Ga | ppm | 20.10 | 19.6 | 20.7 | 19.4 | 18.1 |
| Hf | ppm | 6.40 | 6.5 | 6.4 | 5 | 6.8 |
| Nb | ppm | 35.00 | 33.5 | 33.2 | 26.7 | 42.1 |
| Rb | ppm | 274.80 | 269.6 | 309.6 | 238.5 | 305.1 |
| Sn | ppm | 3.00 | 2 | 3 | 3 | 4 |
| Sr | ppm | 903.00 | 889.4 | 919.8 | 946 | 724.7 |
| Ta | ppm | 1.80 | 1.8 | 1.8 | 1.4 | 2.3 |
| Th | ppm | 22.10 | 24.2 | 22.8 | 18.1 | 29.7 |
| U | ppm | 6.80 | 6.8 | 6.1 | 5.2 | 9 |
| V | ppm | 193.00 | 190 | 209 | 208 | 110 |
| W | ppm | 4.00 | 4 | 3.5 | 4.6 | 6.5 |
| Zr | ppm | 233.20 | 229.6 | 229.2 | 182 | 267.9 |
| Y | ppm | 32.50 | 31.8 | 33.4 | 28.7 | 32.1 |
| La | ppm | 64.10 | 63.6 | 63.7 | 56 | 74.3 |
| Ce | ppm | 123.60 | 121.7 | 123.8 | 109.7 | 139.6 |
| Pr | ppm | 13.40 | 13.39 | 13.74 | 12.37 | 14.82 |
| Nd | ppm | 53.90 | 53.3 | 56.8 | 49.2 | 57 |
| Sm | ppm | 10.10 | 10 | 10.5 | 9.7 | 9.9 |
| Eu | ppm | 2.37 | 2.28 | 2.5 | 2.24 | 2.27 |
| Gd | ppm | 7.66 | 7.37 | 7.78 | 6.99 | 7.14 |
| Tb | ppm | 1.08 | 1.05 | 1.1 | 1.03 | 1.04 |
| Dy | ppm | 5.89 | 5.85 | 5.97 | 5.47 | 5.65 |

Table 2 (*continued*)

| | | CF-FR-C1 | RE CF-FR-C1 | CF-FR-C2 | CF-MI1-C1 | CF-MI1-C2 |
|---|---|---|---|---|---|---|
| Ho | ppm | 1.08 | 1.06 | 1.07 | 0.99 | 1.07 |
| Er | ppm | 2.89 | 2.9 | 2.95 | 2.68 | 2.95 |
| Tm | ppm | 0.45 | 0.42 | 0.44 | 0.38 | 0.46 |
| Yb | ppm | 2.48 | 2.6 | 2.63 | 2.41 | 2.65 |
| Lu | ppm | 0.41 | 0.41 | 0.42 | 0.36 | 0.41 |

*=FeO by dichromate titration.

These trends are consistent with crystallization of olivine and clinopyroxene from alkali basalt magma. In particular, the trends described above suggest earlier crystallization of olivine in the CF-FR-C1 sample and clinopyroxene in the CF-FR-C2 sample compared with the timing of crystallization of clinopyroxene in the CF-FR-C1 scoria sample. The $TiO_2$ contents of these MI are consistent with the low Ti-contents of lavas from the Roman Comagmatic Province. To explain Ti enrichment in the bulk rock compared with MI (whose compositions should represent the melt composition before the eruption), the studied rocks would have to contain about 60% groundmass and ≈40% phenocrysts (clinopyroxene, olivine, feldspar and biotite), which is a higher phenocryst abundant than that observed in thin sections. If we assume that the groundmass has a composition similar to MI in more evolved clinopyroxene, then $TiO_2$ bulk-rock contents are compatible with analyzed values (Tables 1a–c).

It is more difficult to explain $Na_2O$ enrichment in the bulk rock, even though $Na_2O$ in the melt is expected to increase during crystallization (Na behaves as an incompatible element during magma fractionation). We also observe a greater Na enrichment in Fondo Riccio bulk rock compared to Minopoli1 bulk rock (Table 2). Hydrothermal activity is present in the vicinity of the Fondo Riccio eruption and, as explained for similar behavior at Vesuvius (Lima et al., this volume), $Na_2O$ enrichment in the bulk rock most likely represents the effects of hydrothermal fluids. During explosive eruptions associated with decompression during magma ascent, the reaction of NaCl with $H_2O$ at low pressure (<300 bars) becomes important and hydrolysis reactions produce HCl and NaOH that remain preferentially in the melt (Veksler, 2004). Note that the trend in Na enrichment observed here is the opposite of that observed during subsolidus hydrothermal alteration of melt inclusions in porphyry copper systems (Student and Bodnar, 2004).

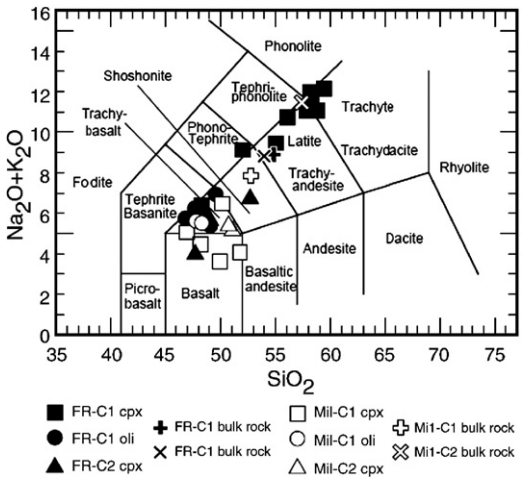


Fig. 4. Total alkali–silica diagram (Le Bas et al., 1986) showing compositions of MI hosted in clinopyroxene and olivine from Fondo Riccio and Minopoli 1. Bulk-rock compositions are also shown.

The volatile content of MI as a function of $SiO_2$ for the two eruptions are shown in Fig. 6. The $SO_2$ content of MI in clinopyroxene from scoria (C1) varies between 0.04 and 0.29 wt.%; and from 0.25 to 0.40 wt.% for MI in olivine from the scoria (C1) and from 0.13 to 0.34 wt.% for MI in clinopyroxene from the bomb (C2). For Minopoli 1 MI, $SO_2$ varies from 0.09 to 0.11 wt.% for clinopyroxene from C1, from 0.21 to 0.34 wt.% for MI in olivine from C1, and from 0.31 to 0.37 wt.% for MI in clinopyroxene from C2. The $SO_2$ concentration decreases with increasing $SiO_2$, consistent with degassing during magma crystallization. MI hosted in clinopyroxene from FR-C1 shows little variation in S content as a function of $SiO_2$. One Minopoli 1 MI containing approximately 48 wt.% $SiO_2$ and 0.91 wt.% $SO_2$ falls well outside the range of all other values. This data point was not discarded because it represents the average of two nearly identical analyses on the same MI.

Decreasing $P_2O_5$ with increasing $SiO_2$ (Fig. 6b) is consistent with apatite crystallization during magma evolution. No systematic variation in F is observable for the two samples (Fig. 6c).

Chlorine abundance (Fig. 6d) in the Fondo Riccio MI ranges from 0.32 to 0.72 wt.% in MI in clinopyroxene from the scoria (mean of 0.54 wt.%), whereas Cl shows

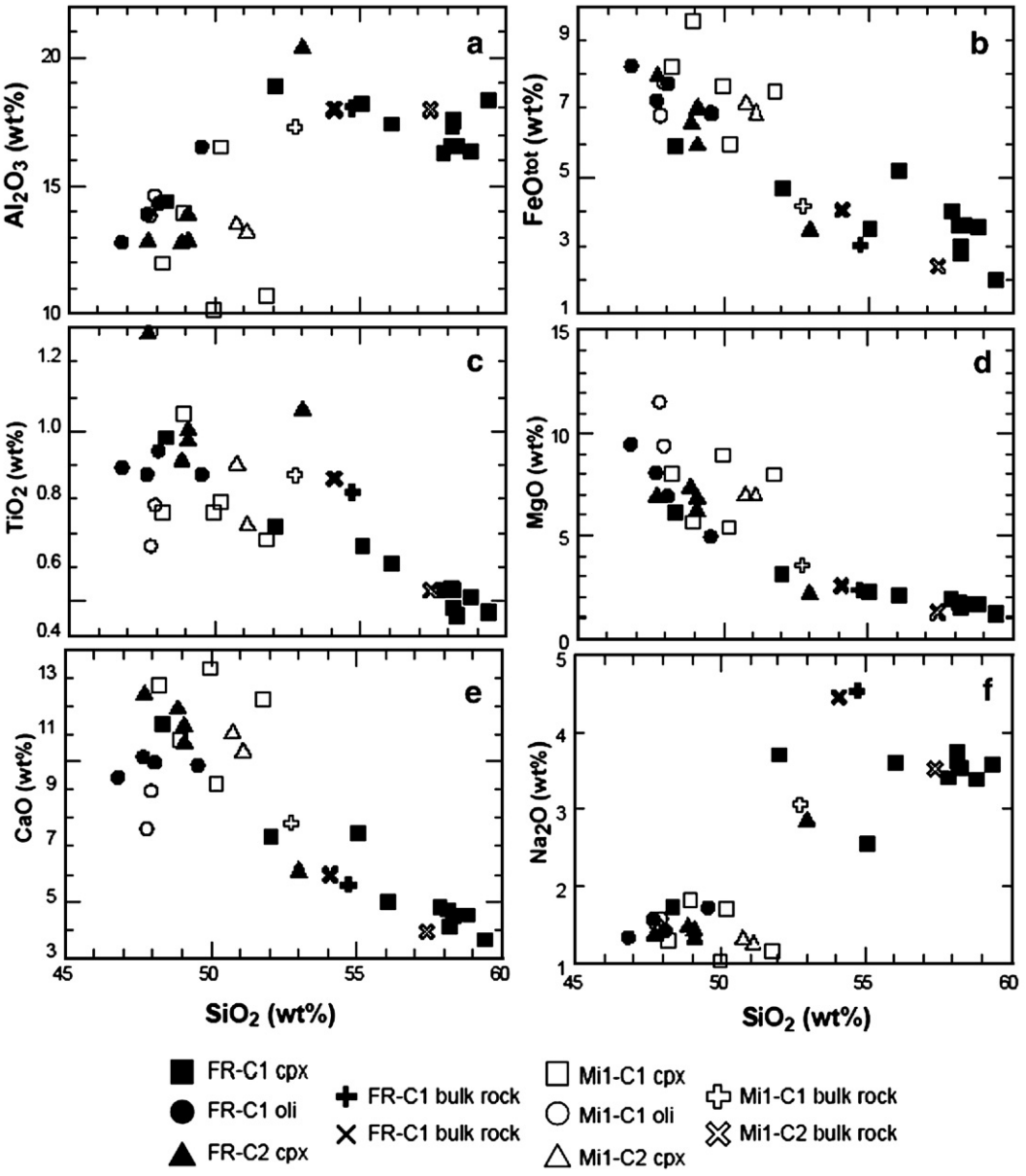


Fig. 5. Harker variation diagrams for MI plotted versus $SiO_2$: (a) $Al_2O_3$; (b) $FeO^{tot}$; (c) $TiO_2$; (d) MgO; (e) CaO; (f) $Na_2O$.

much less variation in MI in clinopyroxene from the bomb sample (CF-FR-C2) (between 0.42 and 0.57 wt.% with a mean of 0.49 wt.%) and in MI in olivine from CF-FR-C1 sample (between 0.42 and 0.47 wt.% with a mean of 0.44 wt.%). Minopoli 1 MI shows a smaller variation in Cl content compared to Fondo Riccio. Cl varies from 0.34 to 0.2 wt.% in MI in clinopyroxenes from Mi1-C1 (mean 0.27 wt.%), 0.43±0.01 wt.% for MI in olivine from Mi1-C1 and from 0.39 to 0.42 wt.% for MI in clinopyroxene from Mi1-C2. These results suggest that the magma that generated the Fondo Riccio scoria phenocrysts was not affected by Cl loss. The Cl content is slightly higher in more evolved MI than in less evolved MI for Fondo Riccio samples (Fig. 6d), whereas such a trend is not observed for Minopoli 1 MI.

The average $H_2O$ content, measured by EMPA, is consistent with the $H_2O$ obtained by SIMS (Fig. 7). In general, less evolved MIs have higher concentrations of water and Fondo Riccio MI are enriched in $H_2O$ compared to Minopoli 1 MI (even though the

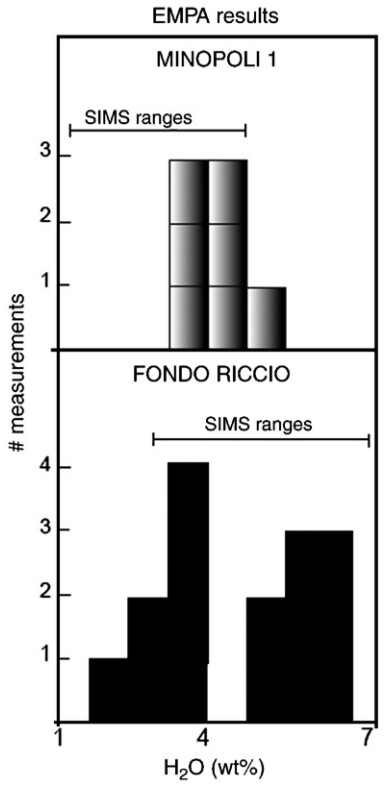


Fig. 6. Water contents of MI obtained by EMPA and SIMS.

concentrations overlap). This may explain the more explosive character of the Fondo Riccio eruption compared to the Minopoli 1 eruption.

In order to better understand the origin of the magma that fed these two eruptions, trace element systematics have been examined. Compositions of MI from both eruptions have B and Be concentrations that fall close to the B/Be=4 line that divides rocks that originate in volcanic arc environments and those that are sourced in an ocean island volcanic setting (Fig. 8). Rb versus Y+Nb systematics of MI straddle the boundary between rocks associated with "within plate" volcanism and those generated in volcanic arc settings (Fig. 9). Y/Nb versus Zr/Nb systematics of MI are consistent with magmas generated in the upper continental crust, but also point towards the island arc environment (Fig. 10). An upper continental crust origin for the MI is also suggested by the Sr, Rb, Th, Nb, Ce, Zr, Sm, Y and Yb spider diagram (Pearce et al., 1983) (Fig. 11).

The relationship between Rb and Cs for MI from Somma–Vesuvius (SV) and the Campanian Ignimbrite (CI) (shaded areas) from Webster et al., 2003 are compared with MI from this study in Fig. 12. The data suggest that Fondo Riccio and Minopoli 1 eruptive products were more likely generated from a magma similar to that which fed Somma–Vesuvius rather than that which produced the Campanian Ignimbrite rocks.

The trace element data presented above are consistent with the tectonic setting of the Neapolitan area, and with

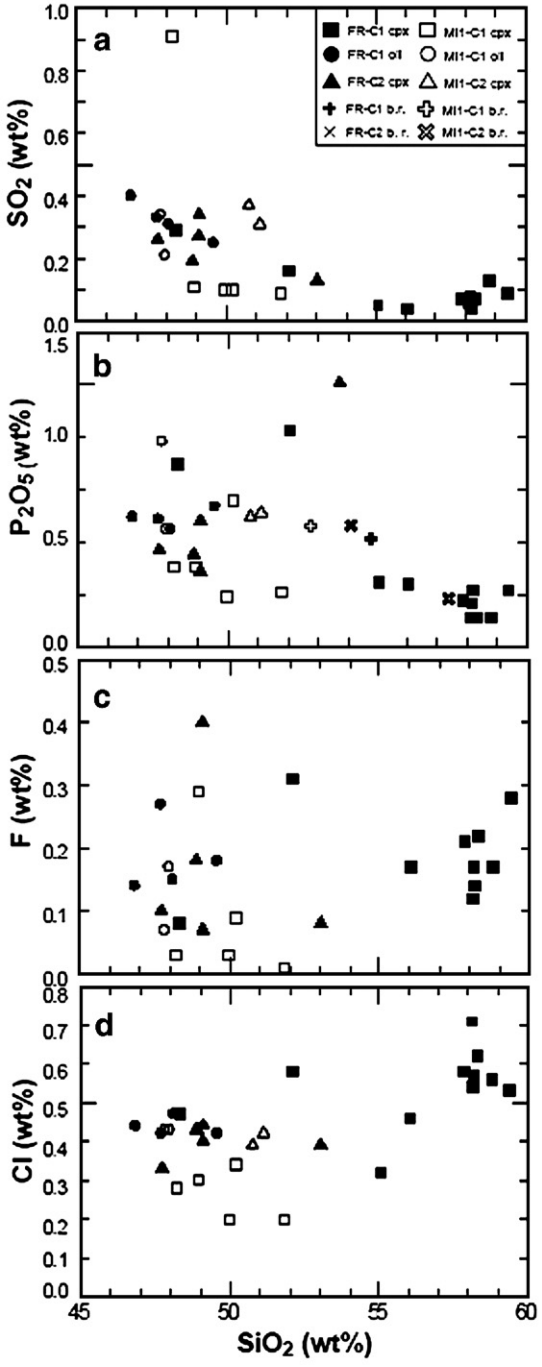


Fig. 7. Volatile concentrations in MI from Fondo Riccio and Minopoli 1 plotted versus $SiO_2$ concentration.

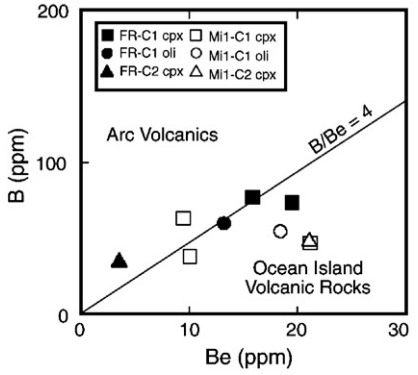


Fig. 8. Relationship between B and Be for Fondo Riccio and Minopoli 1 MI. The diagonal line corresponds to B/Be=4 and divides arc volcanic magmas from ocean island volcanic magmas. Both samples fall along the boundary line, suggesting a mixed arc volcanic and ocean island origin. Two data points for samples Mi1-C1-p6 M2 and FR-C1-o4 M1 have not been plotted.

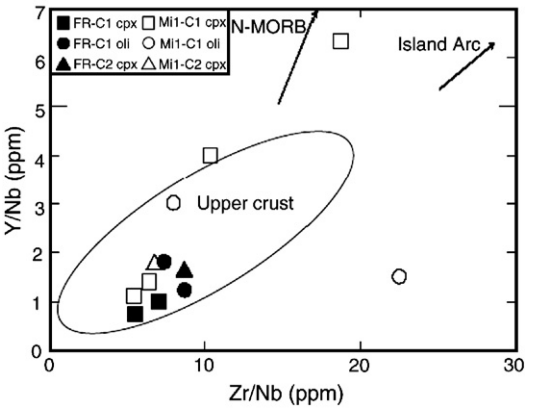


Fig. 10. Relationship between Y/Nb and Zr/Nb for Fondo Riccio and Minopoli 1 MI. Compositions of MI from both samples suggest an upper crustal magma source.

the possible involvement of slab-derived fluids, as suggested by Piochi et al. (2005).

## 5. Conclusions

MIs from Fondo Riccio and Minopoli 1 show systematic variations in composition compared to the bulk-rock compositions. Major and trace element compositions of MI are consistent with an evolving magma chamber in which olivine and clinopyroxenes are crystallizing. The composition of MI in olivine from Fondo Riccio scoria (CF-FR-C1) is similar to MI in clinopyroxene from the bomb (CF-FR-C2). Except for clinopyroxene in Fondo Riccio C1, MI are generally less evolved than the corresponding host rock. Major and trace elements in Fondo Riccio MI show a wider variation compared to those in Minopoli 1 MI. This could be interpreted to indicate that the Fondo Riccio magma residence time was longer compared to the Minopoli 1 magma. $Na_2O$ enrichment in the Fondo Riccio bulk rock represents the effects of hydrothermal activity in the volcanic system before and during the explosive eruptions (see, De Vivo and Lima, 2005; Lima et al., this volume).

The concentration of $SO_2$ and $H_2O$ is higher in less evolved MI, whereas Cl is higher in more evolved MI. F shows no obvious variation as a function of $SiO_2$. The generally higher volatile contents of Fondo Riccio MI are consistent with the more explosive character of this eruption compared to Minopoli 1. Trace element data suggest a combination of arc volcanic and upper continental crust magma as the source for the Fondo Riccio and Minopoli 1 eruptions. Major and trace element

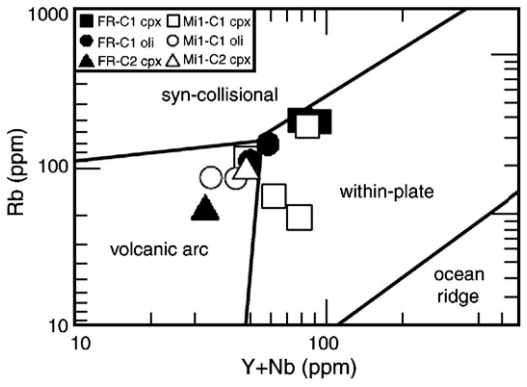


Fig. 9. Relationship between Rb and Y+Nb for Fondo Riccio and Minopoli 1 MI. MI compositions are near the boundary between the volcanic arc and "within plate" fields, suggesting a mixed magma source (see also Fig. 1 in Piochi et al., 2005).

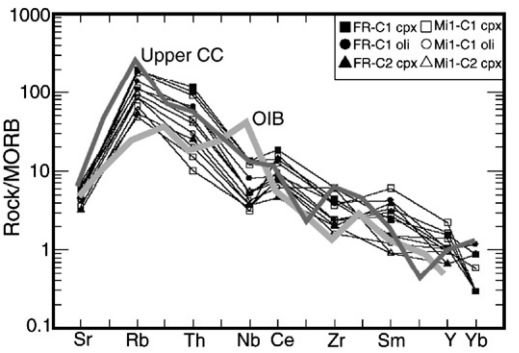


Fig. 11. Spider diagram for Fondo Riccio and Minopoli 1 MI (Pearce, 1983). The heavier lines show the upper continental crust (Upper CC) and the oceanic island basalt (OIB) trends.

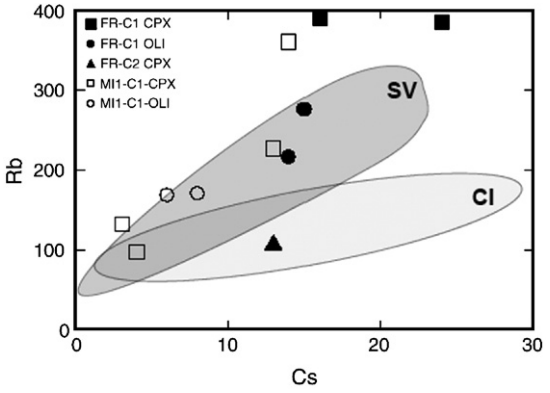


Fig. 12. Relationship between Rb and Cs for Fondo Riccio and Minopoli 1 MI. The data suggest that the feeding mechanism of these two eruptions is more similar to the Somma–Vesuvius (SV) magma source than the Campanian Ignimbrite source.

systematics suggest that these two eruptions, which occurred at different times, were sourced from a single batch of magma that has evolved with time. The smaller range in compositions of the Minopoli 1 MI compared to the Fondo Riccio samples suggests a shorter residence time for Minopoli compared to Fondo Riccio magma.

## Acknowledgements

The authors are grateful to M. Piochi (INGV, Napoli) for the support given to C. Cannatelli during field sampling. The research benefited from funds of the Dottorato Internazionale "Dinamica Interna dei Sistemi Magmatici di Vulcani Attivi" (2004–2006), approved by MIUR, between University of Napoli Federico II (Coordinator: Prof. B. De Vivo) and Virginia Tech (Coordinator: Prof. R. J. Bodnar). We appreciated reviews by N. Metrich and an anonymous referee that helped to improve the final version of the manuscript. Suggestions and comments by Dr. Wendy Bohrson improved our understanding of magma evolution in volcanic systems.

## References

Anderson, A.T., 1974. Chlorine, sulfur and water in magmas and oceans. Geol. Soc. Amer. Bull. 85, 1485–1492.

Anderson, A.T., 1976. Magma mixing: petrological process and volcanological tool. J. Volcanol. Geotherm. Res. 1, 3–33.

Anderson, A.T., 2003. An introduction to melt (glass±crystals) inclusions. Fluid Inclusions. Analysis and Interpretations. Min. Assoc. Canada, vol. 32, p. 374.

Barberi, F., Cassano, E., La Torre, P., Sbrana, A., 1991. Structural evolution of Campi Flegrei Caldera in light of volcanological and geophysical data. J. Volcanol. Geotherm. Res. 48 (1/2), 33–49.

Belkin, H.E., De Vivo, B., Roedder, E., Cortini, M., 1985. Fluid inclusions geobarometry from ejected Mt. Somma-Vesuvius nodules. Am. Mineral. 70, 288–303.

Burnham, C.W., 1979. The importance of volatile constituents. The Evolution of the Igneous Rocks; 50th Anniversary Perspective. Princeton University Press, pp. 439–482.

Carroll, M.R., Holloway, J.R., 1994. Volatiles in magma. Mineral. Soc. Am. Rev. Mineral 30.

Clocchiatti, R., 1975. Les inclusions vitreuses des cristaux de quartz, Etude optique, thermooptique et chemique, Applications geologiques. Soc.Geol.France, Memoires, New Series, vol. 122. 96 pp.

Cundari, A., Fergusson, A.K., 1982. Significance of the pyroxene chemistry from leucite-bearing rocks and related assemblages. Tschermaks. Mineral. Petrogr. Mitt. 30, 189–204.

Danyushevsky, L.V., Della Pasqua, F.N., Sokolov, S., 2000. Re-equilibration of melt inclusions trapped by magnesian olivine phenocrysts from subduction-related magmas: petrological implications. Contrib. Mineral. Petrol. 138, 68–83.

D'Antonio, M., Civetta, L., Di Girolamo, P., 1999. Mantle source heterogeneity in the Campanian Region (South Italy) as inferred from geochemical and isotopic features of mafic volcanic rocks with shoshonitic affinity. Mineral. Petrol. 67, 163–192.

D'Argenio, B., Pescatore, T., Scandone, P., 1973. Schema geologico dell'Appennino Meridionale (Campania e Lucania). Moderne Vedute della Geologia dell'Appennino, Accad. Nazl. dei Lincei, Roma, Italy, p. 183.

Deino, A.L., Orsi, G., de Vita, S., Piochi, M., 2004. The age of the Neapolitan Yellow Tuff caldera-forming eruption (Campi Flegrei caldera—Italy) assessed by $^{40}Ar/^{39}Ar$ dating method. J. Volcanol. Geotherm. Res. 133, 157–170.

De Vivo, B., Lima, A., 2005. A hydrothermal model for ground movements (bradyseism) at Campi Flegrei, Italy. In: De Vivo, B. (Ed.), Volcanism in the Campania Plain: Vesuvius, Campi Flegrei and Ignimbrites. Developments in Volcanology, vol. 9. Elsevier.

De Vivo, B., Rolandi, G., Gans, P.B., Calvert, A., Bohrson, W.A., Spera, F.J., Belkin, H.E., 2001. New constraints on the pyroclastic eruptive history of the Campanian volcanic Plain (Italy). Mineral. Petrol. 73, 121–143.

Di Girolamo, P., Ghiara, M.R., Lirer, L., Munno, R., Rolandi, G., Stanzione, D., 1984. Vulcanologia e Petrologia dei Campi Flegrei. Boll. Soc. Geol. Ital. 103, 349–413.

Di Vito, M.A., Lirer, L., Mastrolorenzo, G., Rolandi, G., 1987. The 1538 Monte Nuovo eruption (Campi Flegrei, Italy). Bull. Volcanol. 49 (4), 608–615.

Di Vito, M.A., Isaia, R., Orsi, G., Southon, J., D'Antonio, M., de Vita, S., Pappalardo, L., Piochi, M., 1999. Volcanic and deformation history of the Campi Flegrei caldera in the past 12 ka. J. Volcanol. Geotherm. Res. 91, 221–246.

Doglioni, C., 1991. A proposal for kinematic modeling of W dipping subductions. Possible applications to the Tyrrhenian–Apennines system. Terra Nova 3, 426–434.

Fedele, L., Bodnar, R.J., DeVivo, B., Tracy, R.J., 2003. Melt inclusion geochemistry and computer modeling of trachyte petrogenesis at Ponza, Italy. Chem. Geol. 194, 81–104.

Frezzotti, M.L., 2001. Silicate–melt inclusions in magmatic rocks: application to petrology. Lithos 55, 273–299.

Gvirtzman, Z., Nur, A., 2001. Residual topography, lithospheric structure and sunken slabs in the central Mediterranean. Earth Planet. Sci. Lett. 187, 117–130.

Hippolyte, J.C., Angelier, J., Roure, F., 1994. A major geodynamic change revealed by Quaternary stress patterns in the Southern Apennines. Tectonophysics 230, 199–210.

Ippolito, F., D'Argenio, B., Pescatore, T., Scandone, P., 1975. Structural-stratigraphic units and tectonic framework of Southern Apennines. In: Squyres, C. (Ed.), Geology of Italy. Lybian Soc. of Earth Sci. Press, Libyan Arab Republic, Tripoli, pp. 317–328.

Le Bas, M.J., Le Maitre, R.W., Streckeisen, A., Zanettin, B., 1986. A chemical classification of volcanic rocks based on the total alkali–silica diagram. J. Petrol. 27, 745–750.

Lima, A., 2000. Experimental study in silicate melt inclusions in clinopyroxene phenocrysts from Roccamorfina lavas (Italy). Mineral. Petrol. 70, 199–220.

Lima A., De Vivo B., Fedele L., Sintoni M.F. (this volume). Geochemical variations between the 79 AD and 1944 AD Mt. Somma–Vesuvius volcanic products: constraints on the evolution of the hydrothermal system based on fluid and melt inclusions. Chem. Geol.

Lowenstern, J.B., 1994. Dissolved volatile concentrations in ore-forming magma. Geology 22, 893–896.

Marianelli, P., Metrich, N., Sbrana, A., 1999. Shallow and deep reservoir involved in magma supply of the 1944 eruption of Vesuvius. Bull. Volcanol. 61, 48–63.

Meletti, C., Patacca, E., Scandone, P., 2000. Construction of a seismotectonic model: the case of Italy. Pure Appl. Geophys. 157, 11–35.

Morgan, G.B., London, D., 1996. Optimizing the electron microprobe analysis of hydrous alkali aluminosilicate glasses. Am. Mineral. 81, 1176–1185.

Morimoto, N., 1988. Nomenclature of pyroxenes. Mineral. Mag. 52, 535–550.

Orsi, G., de Vita, S., Di Vito, M., 1996. The restless, resurgent Campi Flegrei nested caldera (Italy): constraints on its evolution and configuration. J. Volcanol. Geotherm. Res. 74, 179–214.

Pappalardo, L., Civetta, L., D'Antonio, M., Deino, A.L., Di Vito, M.A., Orsi, G., Carandente, A., de Vita, S., Isaia, R., Piochi, M., 1999. Chemical and isotopical evolution of the Phlegraean magmatic system before the Campanian Ignimbrite (37 ka) and the Neapolitan Yellow Tuff (12 ka) eruptions. J. Volcanol. Geotherm. Res. 91, 141–166.

Pappalardo, L., Piochi, M., D'Antonio, M., Civetta, L., Petrini, R., 2002. Evidence for multi-stage magmatic evolution during the past 60 ka at Campi Flegrei (Italy) deduced from Sr, Nd and Pb isotope data. J. Petrol. 43, 1415–1434.

Pearce, J.A., Harris, B.W., Tindle, A.G., 1983. Trace element discrimination diagrams for the tectonic interpretation of granitic rocks. J. Petrol. 25, 956–983.

Peccerillo, A., 1999. Multiple mantle metasomatism in central-southern Italy: Geochemical effects, timing and geodynamic implications. Geology 27, 315–318.

Piochi, M., Bruno, P.P., De Astis, G., 2005. Relative roles of rifting tectonics and magma ascent processes: inferences from geophysical, structural, volcanological, and geochemical data for the Neapolitan volcanic region (southern Italy). Geochem. Geophys. Geosyst. 6 (7).

Piromallo, C., Morelli, A., 1997. Imaging the Mediterranean upper mantle by P-wave travel time tomography. Ann. Geophys. 40, 963–979.

Roedder, E., 1979. Origin and significance of magmatic inclusions. Bull. Mineral. 102, 487–510.

Roedder, E., 1984. Fluid inclusions. Reviews Mineral. Mineral. Soc. Am., Washington D.C., vol. 12. 644 pp.

Rolandi, G., Bellucci, F., Heizler, M.T., Belkin, H.E., De Vivo, B., 2003. Tectonic controls on the genesis of ignimbrites from the Campanian Volcanic Zone, southern Italy. Mineral. Petrol. 79, 3–31.

Rosi, M., Sbrana, A., 1987. Phlegrean fields. CNR, Quaderni de "La Ricerca Scientifica" 114, 1–175.

Scandone, P., 1979. Origin of the Tyrrhenian Sea and Calabrian. Arc. Boll. Soc. Geol. Ital. 8, 27–34.

Selvaggi, G., Amato, A., 1992. Subcrustal earthquakes in the Northern Apennines (Italy): evidence for a still active subduction? Geophys. Res. Lett. 19, 2127–2130.

Selvaggi, G., Chiarabba, G., 1995. Seismicity and P-wave velocity image of the southern Tyrrhenian subduction zone. Geophys. J. Int. 121, 818–826.

Serri, G., Innocenti, F., Manetti, P., 1993. Geochemical and petrological evidence of the subduction of delaminated Adriatic continental lithosphere in the genesis of the Neogene–Quaternary magmatism of central Italy. Tectonophysics 223, 117–147.

Shimizu, N., Hart, S.R., 1982. Application of the ion probe to geochemistry and cosmochemistry. Annu. Rev. Earth Planet. Sci. 10, 483–526.

Sobolev, A.V., 1996. Melt inclusions in minerals as a source of principle petrological information. Petrology 4, 209–220.

Sobolev, A.V., Slutskii, A.B., 1984. Composition and crystallization conditions of the initial melt of the Siberian meimechites in relation to the general problem of ultrabasic magmas. Sov. Geol. Geophys. 25, 93–104.

Sobolev, A.V., Kamenetsky, V.S., Metrich, N., Clocchiatti, R., Koronova, N.N., Devirts, A.L., Ustinov, V.I., 1990. Volatile regime and crystallization conditions in Etna hawaiite lavas. Geochem. Int. 53–65.

Student, J.J., Bodnar, R.J., 2004. Silicate melt inclusions in porphyry copper deposits: identification and homogenization behavior. Can. Mineral. 42, 1563–1600.

Thomas, J.B., Bodnar, R.J., 2002. A technique for mounting and polishing melt inclusions in small (>1 mm) crystals. Am. Mineral. 87 (10), 1505–1508.

Thomas, J.B., Bodnar, R.J., Shimizu, N., Sinha, A.K., 2002. Determination of zircon/melt trace element partition coefficients from SIMS analysis of melt inclusions in zircon. Geochim. Cosmochim. Acta 66, 2887–2902.

Tonarini, S., Leeman, W.P., Civetta, L., D'Antonio, M., Ferrara, G., Necco, A., 2004. B/Nb and $\delta^{11}$B systematics in the Phlegraean volcanic district, Italy. J. Volcanol Geotherm. Res. 133, 123–139.

Veksler, I.V., 2004. Liquid immiscibility and its role at magmatic–hydrothermal transition: a summary of experimental studies. Geoch. Geol. 210, 7–31.

Wallace, P.J., 2005. Volatiles in subduction zone magmas; concentrations and fluxes based on melt inclusion and volcanic gas data. J. Volcanol. Geotherm. Res. 140 (1–3), 217–240.

Webster, J.D., Burt, D.M., Aguillon, R.A., 1996. Volatile and lithophile trace-element geochemistry of heterogeneous Mexican tin rhyolite magmas deduced from compositions of melt inclusions. Geochim. Cosmochim. Acta 60, 3267–3283.

Webster, J.D., Raia, F., De Vivo, B., Rolandi, G., 2001. The behavior of chlorine and sulfur during differentiation of the Mt. Somma–Vesuvius magmatic system. Mineral. Petrol. 73, 177–201.

Webster, J.D., Raia, F., Tappen, C., De Vivo, B., 2003. Pre eruptive geochemistry of the ignimbrite-forming magmas of the Campanian Volcanic Zone, Southern Italy, determined from silicate melt inclusions. Mineral. Petrol. 79, 99–125.